GENERAL REWIEV

UDC: 616.1-08::616.132.2-004.6
DOI: 10.2298/VSP150809139S

Atherosclerosis and coronary artery bifurcation lesions: anatomy and flow characteristics

Ateroskleroza račvi koronarnih arterija: anatomske i hemodinamske karakteristike

Goran Stanković*†‡, Vladan Vukčević*†, Miroslav Živković§, Zlatko Mehmedbegović*, Milorad Živković*, Vladimir Kanjuh‡

***Department of Cardiology, Clinical Center of Serbia, Belgrade, Serbia; †Faculty of Medicine, University of Belgrade, Belgrade, Serbia; ‡Serbian Academy of Sciences and Arts, Belgrade, Serbia; §Faculty of Mechanical Engineering, Kragujevac, Serbia**

Key words:
coronary vessels; coronary disease; atherosclerosis; angioplasty, baloon, coronary.

Ključne reči:
koronarni krvni sudovi; koronarna bolest; arterioskleroza; angioplastika, translumenska, perkutana, koronarna.

Introduction

Although the coronary arterial tree is uniformly exposed to the systemic risk factors, we have learned since the beginning of the 20th century that atherosclerotic "plaques" preferentially develop at vessel branch points [1–3]. As a result, coronary bifurcations in recent reports account for 15–20% of all percutaneous coronary interventions (PCI) [4–6]. Coronary artery bifurcations are predilection sites for atherosclerosis development as a result of specific flow characteristics and local endothelial shear stress (ESS) presentation [7]. Anatomic features of coronary bifurcations, such as diameter of the main vessel (MV) and the side branches (SB), atherosclerotic plaque burden in the proximal and distal part of the MV and the SB, and bifurcation angle, all impact on local flow patterns [8]. The relationship among the coronary anatomy, local flow and vascular biology promotes the progression and complexity of atherosclerosis in coronary bifurcations. The complex local hemodynamic microenvironment after bifurcation stenting also influences in-stent restenosis, thrombosis and clinical outcomes [9].

In this review, we summarized the current data with respect to coronary artery bifurcation anatomy and flow characteristics, the impact of local hemodynamic conditions in initiation and progression of atherosclerosis and application of this basic knowledge in contemporary PCI.

Fractal geometry of coronary artery bifurcations

Ramifications of the coronary tree follow the natural law of conservation of mass and minimum energy expenditure in providing underlying myocardium with the optimum amount of blood [8, 10]. According to the law of conservation of mass, the flow (Q) through the proximal, "mother" segment of the MV must equal the sum of the flow through the two "daughter" vessels (specifically, distal part of the MV and the SB, Figure 1) [8]. Since flow is related to the lumen cross-sectional area and flow velocity, there is a relation between the function (blood flow) and anatomy or geometry (cross-sectional diameter and area) [4, 6]. There are many theories of the vascular tree design based on the concept of minimum work. Murray's law (also known as the "cube law"), is based on a minimum energy hypothesis, and states that the sum of the cubes of the "daughter" vessel diameters ($D_{daughter1}$ and $D_{daughter2}$) is equal to the cube of the "mother" vessel diameter (D_{mother}) as : $D_{mother}^3=D_{daughter1}^3+D_{daughter2}^3$ (Figure 1) [8]. Finet et al. [8] show that Murray's law cannot be applied in the entire coronary tree and suggest a $^{7/3}$ exponent in their HK model: $D_{mother}^{7/3}=D_{daughter1}^{7/3}+D_{daughter2}^{7/3}$. Finally, Finet et al. [8] (Figure 1) proposed a linear relation ($D_{mother}=0.678*[D_{daughter1}+D_{daughter2}]$) based on regression analysis of Y-type bifurcation (where 0.678 expresses the ratio of the "mother" vessel diameter to the sum of two "daughter" vessel diameters) [8].

Correspondence to: Goran Stanković, Department of Cardiology, Clinical Center of Serbia, Višegradska 26, 11 000 Belgrade, Serbia. Phone: +381 11 362 90 56. E-mail: gorastan@sbb.rs

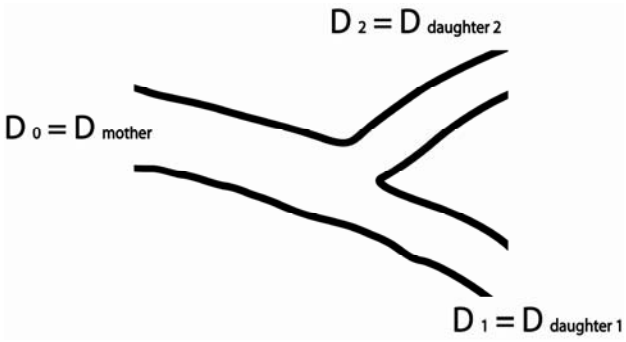

Fig. 1 – Fractal anatomy of coronary artery bifurcation scheme. The mother vessel divides into two daughter vessels and the diameter of the mother vessel (D_0) is greater than any of the two daughter vessel diameters (D_1 and D_2).

Therefore, coronary tree does not taper linearly and change in diameter occurs predominantly at bifurcation points. As a consequence, each bifurcation consists of three segments with different diameters which have the fractal geometry, with a constant relation between diameters defined by the scaling laws [5–8]. The proximal "mother" segment of the MV is consequently always larger in diameter compared to the distal segments (Figure 2), and equals (according to fractal ratio equation) approximately two thirds of the sum of two "daughter" vessels diameters [10]. This natural fractal law has to be kept in mind for optimal selection of material for PCI.

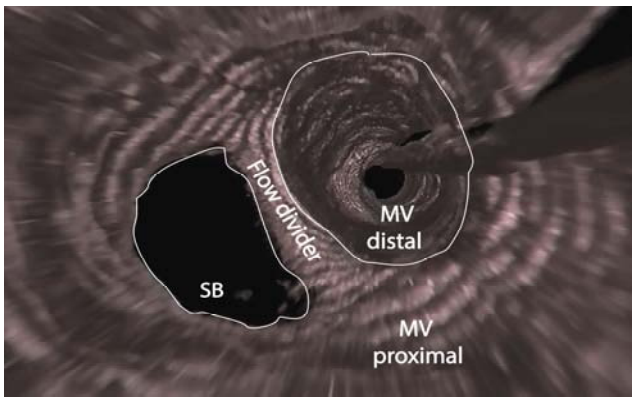

Fig. 2 – 3D optical coherence tomography pullback reconstruction, showing a larger proximal main vessel (MV) diameter and smaller distal MV and side branch (SB) diameters, separated by a flow divider.

Flow distribution in coronary bifurcations

ESS is the tangential force applied to the luminal endothelial layer, which is caused by the friction of blood flow and is expressed in units of force / unit area [2]. Arterial bifurcations are known for their characteristic flow velocity patterns resulting in flow separation, recirculation and secondary flow patterns leading to local low and oscillatory ESS along the lateral walls, while high ESS develops in the flow divider (carina) of the bifurcation (Figure 3) [7, 11–14]. The proportion of flow directed towards the SB determines the ESS patterns within the bifucration [2]. Computational flow dynamic studies acknowledged different patterns of flow and the impact of anatomic variations in the flow profile in coronary bifurcations [13, 15]. Furthermore, *in vitro* studies show that bifurcation angle and diameter also play an important role in local ESS patterns, and wider angles and larger vessel diameters create a greater turbulence in flow and consequently create lower ESS [16]. Finaly, the ratio between the MV and the SB diameters influences flow hemodynamic profile [17].

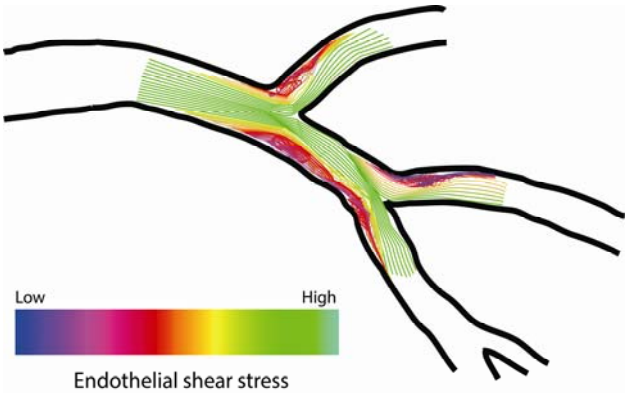

Fig. 3 –Endotelial shear stress distribution in coronary artery bifurcation illustrating low values at the lateral walls and high values at the carina.

Further complexity of hemodynamic profile is introduced by temporal alterations in ESS caused by flow pulsatility [18]. A typical temporal pattern is characterized by low and oscillatory ESS during heart systole and rapid increase and then slow decrease during diastole [18]. These temporal changes may also have an impact on the process of initiation and progression of atherosclerosis [7, 19].

Atherosclerotic plaque development and progression

In 1969 Caro et al. [20] first associated ESS with atherosclerotic plaque formation. Low or oscillatory ESS promotes plaque formation inside the entire vascular tree and there is a strong correlation between endothelial dysfunction, low shear stress and oscillatory flow, predominantly at sites of bifurcations and at curvatures [2, 13, 14, 21–23]. The mechanism of plaque creation in low ESS areas is very complex but several reports imply that low ESS modulates the molecular, cellular and vascular dynamics, which are responsible for atherogenesis and progression of plaque towards a high-risk phenotype [3, 24, 25]. Endothelial cells have important role because they alter gene expression pattern in response to flow-mediated ESS changes, with consequent activation of pro-atherogenic transcription factors [18]. Shear stress plays an important role not only in early plaque formation but also its progression. Plaque progression is initiated by endothelial dysfunction, with increased permeability for lipoproteins and with up-regulation of adhesion molecules, such as intercellular adhesion molecules 1, vascular cell adhesion molecules and leukocyte transmigration [26, 27].

Histopathology of atherosclerosis in coronary artery bifurcations

Pathologic studies showed that atherosclerosis predominantly involves the outer (lateral) wall of vessel bi-

furcations opposite to carina, which corresponds to low and oscillatory ESS regions (Figure 4) [28–30]. Autopsy studies also describe the presence of intimal thickening in the lateral wall of bifurcation, with the absence of lesion formation at the inner wall (flow divider or carina) [31]. In addition, atherosclerotic lesions were more frequent in autopsy specimens on the myocardial side than on the epicardial side of the arteries [31]. Pathologic studies in swine showed eccentric neointimal hyperplasia at the lateral wall following MV stenting, with concurrent acute adhesion and accumulation of leukocytes, while leukocytes were absent at the carina [17]. Nakazawa et al. [29] determined plaque distribution inside the MV and the SB in patients dying from sudden coronary death [29]. Each bifurcation was morphologically assessed including intimal thickness and necrotic core distribution in the MV (proximal and distal to SB origin), in the SB and at the carina region. Similar to prior reports, lateral walls showed a significantly greater intimal thickness as compared to those in the flow divider region [29]. Plaque thickness was highest at the lateral wall in the distal MV, followed by the lateral wall in the proximal MV. Similarly, advanced atherosclerotic plaques with necrotic core were also significantly greater at the lateral regions as compared with the flow divider area, where necrotic core formation was usually minimal or frequently absent. Interestingly, plaque progression might influence local geometry by increasing lumen obstruction with subsequent flow acceleration. This observation may explain plaque formation at high ESS areas in bifurcations [15].

Fig. 4 – Histologic image of coronary plaque in native bifurcation lesion. Longitudinal section shows necrotic core accompanied with calcification within the plaque predominantly at low endothelial shear stress (ESS) areas (lateral wall oposite to carina), whereas high ESS (flow divider/carina) has minimal intimal thickening.

Autopsy studies following bifurcation stenting showed increased rate of restenosis in patients treated with bare metal stents, a higher risk of late stent thrombosis with drug-eluting stents and similar risk of acute and subacute stent thrombosis (< 30 days) with both stent types [32]. Joner et al. [32] documented differences in the healing patterns in cases with drug-eluting stents as compared with bare metal stents. In cases with drug-eluting stents, delayed vascular healing, with uncovered struts and fibrin deposition were significantly greater at the carina sites compared to the lateral walls and most of the thrombi in these cases originate at the carina sites [32]. It has been demonstrated that low ESS upregulates growth factors and increases local thrombogenicity while high ESS augments platelet activation and aggregation [2, 33].

Importantly, stent design characteristics and the relationship between stent struts and vessel wall influence flow hemodynamics and clinical outcomes [34]. Stents with thicker struts and less streamlined configuration (*ie* rectangular configuration) have higher rates of in-stent restenosis, likely due to the generation of high ESS proximal and above the stent struts and low ESS with flow recirculation downstream (distal) to the struts [2, 9, 35]. Stent overlap aggravates local flow hemodynamics which may have impact on clinical outcomes [36].

Clinical implications

Percutaneous treatment of bifurcation lesion remains technically challenging and still results in higher rates of procedural complications [4]. Based on randomized clinical trials provisional SB stenting is the recommended approach for the majority of bifurcation lesions and with this approach, a single stent can be used in 80–90% of cases with optimal clinical outcome [4, 6]. Application of information on fundamental aspects of coronary bifurcation anatomy and flow characteristics is essential to fully understand the technical approach used for the provisional SB stenting strategy. Procedural planning starts with the analysis of coronary angiography and anticipation of plaque distribution in accordance with the knowledge acquired from pathologic studies (Figures 5A and 5B).

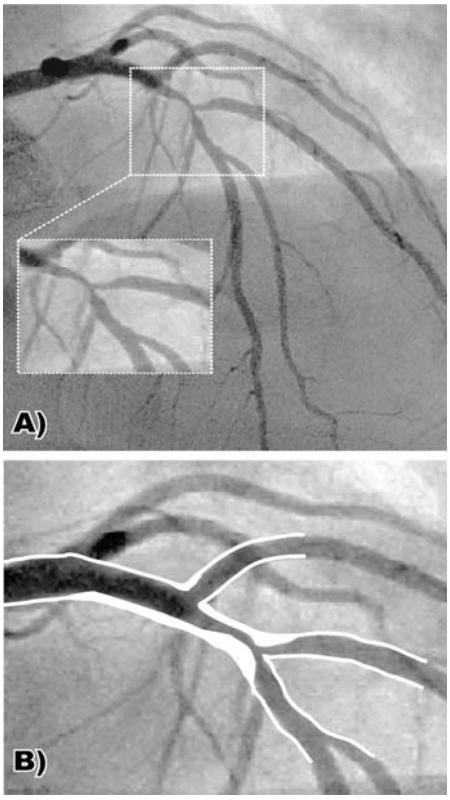

Fig. 5 – A) Coronary angiography of true bifurcation lesion, with significant disease of the main vessel (left anterior descending) and the side branch (diagonal branch); B) Schematic reconstruction of vessel wall and lumen contours, with atherosclerotic plaque area depicted in white.

The procedure begins with MV stenting and, keeping in mind that every bifurcation consists of three segments with different diameters, selection of stent diameter for the MV is crucial. If stent diameter is selected according to the proximal MV reference diameter, it will be oversized for the distal MV and may therefore increase the risk of SB occlusion created by carina shifting [4–6]. Therefore, MV stent diameter should be selected fitting to the distal MV diameter, with understanding that struts will not be opposed in the proximal MV (Figure 6A) [4–6]. Proximal optimization technique is proposed to correct MV stent malapposition by inflating a short bigger balloon and positioning of distal marker at carina (Figure 6B). Residual stenosis in the SB can be treated with different stent implantation techniques, like stenting and small protrusion, internal mini-crush or *culotte*. *Culotte* stenting is characterized by second stent implantation with the overlap in the proximal MV (Figure 7A). The procedure is finalized by the final kissing balloon inflation (Figure 7B). Therefore, application of basic knowledge from pathology and flow analysis allows adjustment of metallic stents to natural fractal anatomy and geometry of bifurcation lesions, especially in bifurcations with large SB, because of a larger difference in the diameters between the proximal and the distal part of the MV.

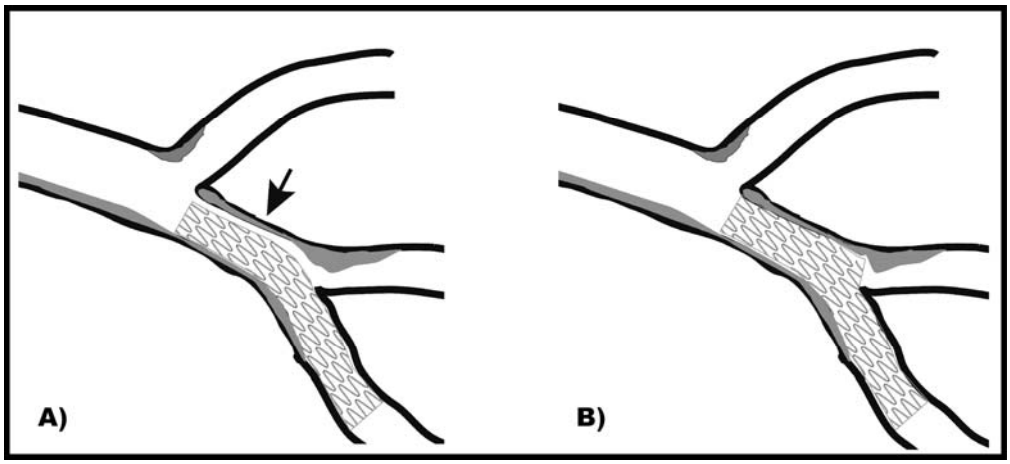

Fig. 6 – A) Schematic presentation of main vessel (MV) stenting, with stent malapposition in the proximal segment of the MV (arrow); B) optimal stent apposition following proximal optimization technique.

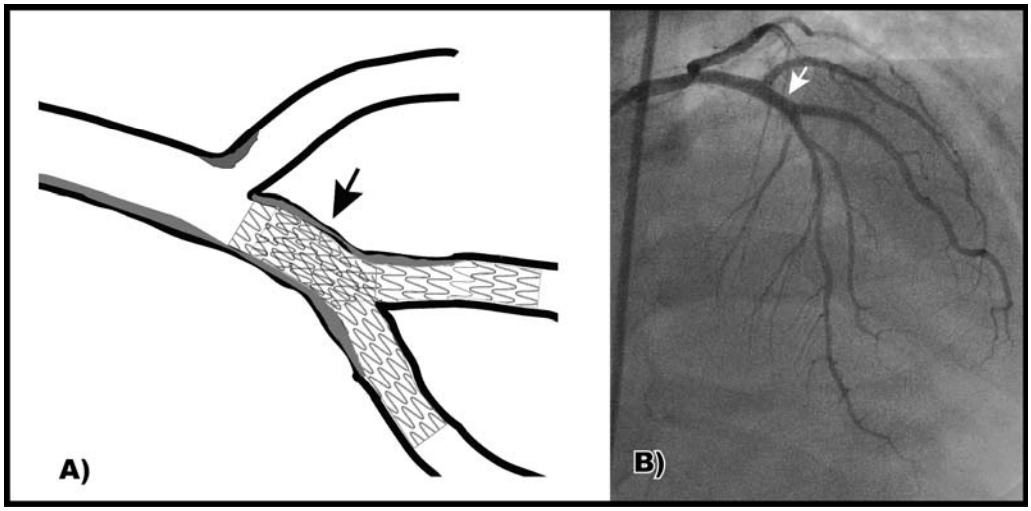

Fig. 7 – A) Schematic presentation of *culotte* stenting technique in lefi anterior descending /diagonal bifurcation, with proximal overlap of the two stents (black arrow); B) final angiographic result following kissing balloon inflation (white arrow).

Conclusion

Coronary bifurcations lesions have particular anatomic and hemodynamic characteristics, which influence the selection of appropriate percutaneous coronary intervention strategy. A complex interaction between the coronary anatomy, local flow characteristics and vascular biology influences development and progression of atherosclerosis in coronary bifurcations. Anticipation of plaque distribution at bifurcation site and application of knowledge from computational fluid dynamic studies allow accurate selection and application of percutaneous coronary intervention strategies.

R E F E R E N C E S

1. *Fry DL*. Certain histological and chemical responses of the vascular interface to acutely induced mechanical stress in the aorta of the dog. Circ Res 1969; 24(1): 93−108.
2. *Chatzizisis YS, Coskun AU, Jonas M, Edelman ER, Feldman CL, Stone PH*. Role of endothelial shear stress in the natural history of coronary atherosclerosis and vascular remodeling: molecular, cellular, and vascular behavior. J Am Coll Cardiol 2007; 49(25): 2379−93.
3. *Chatzizisis YS, Jonas M, Coskun AU, Beigel R, Stone BV, Maynard C*, et al. Prediction of the localization of high-risk coronary atherosclerotic plaques on the basis of low endothelial shear stress: An intravascular ultrasound and histopathology natural history study. Circulation 2008; 117(8): 993−1002.
4. *Lassen JF, Holm NR, Stankovic G, Lefevre T, Chieffo A, Hildick-Smith D,* et al. Percutaneous coronary intervention for coronary bifurcation disease: Consensus from the first 10 years of the European Bifurcation Club meetings. EuroIntervention 2014; 105: 545−60.
5. *Hildick-Smith D, Lassen JF, Albiero R, Lefevre T, Darremont O, Pan M*, et al. Consensus from the 5th European Bifurcation Club meeting. EuroIntervention 2010; 6(1): 34−8.
6. *Stankovic G, Lefevre T, Chieffo A, Hildick-Smith D, Lassen JF, Pan M*, et al. Consensus from the 7th European Bifurcation Club meeting. EuroIntervention 2013; 9(1): 36−45.
7. *Soulis JV, Giannoglou GD, Chatzizisis YS, Farmakis TM, Giannakoulas GA, Parcharidis GE*, et al. Spatial and phasic oscillation of non-Newtonian wall shear stress in human left coronary artery bifurcation: an insight to atherogenesis. Coron Artery Dis 2006; 17(4): 351−8.
8. *Finet G, Huo Y, Rioufol G, Ohayon J, Guerin P, Kassab GS*. Structure-function relation in the coronary artery tree: From fluid dynamics to arterial bifurcations. EuroIntervention 2010; 6 Suppl J: J10−5.
9. *Van der Heiden K, Gijsen FJ, Narracott A, Hsiao S, Halliday I, Gunn J,* et al. The effects of stenting on shear stress: Relevance to endothelial injury and repair. Cardiovasc Res 2013; 99(2): 269−75.
10. *Colombo A, Stankovic G*. Bifurcations and branch vessel stenting. In: *Topol EJ, Teirstein PS,* editors. Textbook of interventional cardiology. 6th ed. Philadelphia: Saunders Elsevier; 2012. p. 270−87.
11. *Giannoglou GD, Soulis JV, Farmakis TM, Giannakoulas GA, Parcharidis GE, Louridas GE*. Wall pressure gradient in normal left coronary artery tree. Med Eng Phys 2005; 27(6): 455−64.
12. *Soulis J, Fytanidis D, Seralidou K, Giannoglou G*. Wall shear stress oscillation and its gradient in the normal left coronary artery tree bifurcations. Hippokratia 2014; 18(1): 12−6.
13. *Blagojevic M, Nikolic A, Zivkovic M, Zivkovic M, Stankovic G*. Influence of blocks' topologies on endothelial shear stress observed in CFD analysis of artery bifurcation. Acta Bioeng Biomech 2013; 15(1): 97−104.
14. *Blagojevic M, Nikolic A, Zivkovic M, Zivkovic M, Stankovic G*. A novel framework for fluid/structure interaction in rapid subject-specific simulations of blood flow in coronary artery bifurcations. Vojnosanit Pregl 2014; 71(3): 285−92.
15. *Gijsen FJ, Schuurbiers JC, van de Giessen AG, Schaap M, van der Steen AF, Wentzel JJ*. 3D reconstruction techniques of human coronary bifurcations for shear stress computations. J Biomech 2014; 47(1): 39−43.
16. *Huo Y, Finet G, Lefevre T, Louvard Y, Moussa I, Kassab GS*. Which diameter and angle rule provides optimal flow patterns in a coronary bifurcation. J Biomech 2012; 45(7): 1273−9.
17. *Richter Y, Groothuis A, Seifert P, Edelman ER*. Dynamic flow alterations dictate leukocyte adhesion and response to endovascular interventions. J Clin Invest 2004; 113(11): 1607−14.
18. *Wentzel JJ, Chatzizisis YS, Gijsen FJ, Giannoglou GD, Feldman CL, Stone PH*. Endothelial shear stress in the evolution of coronary atherosclerotic plaque and vascular remodelling: current understanding and remaining questions. Cardiovasc Res 2012; 96(2): 234−43.
19. *Giannoglou GD, Chatzizisis YS, Zamboulis C, Parcharidis GE, Mikhailidis DP, Louridas GE*. Elevated heart rate and atherosclerosis: An overview of the pathogenetic mechanisms. Int J Cardiol 2008; 126(3): 302−12.
20. *Caro CG, Fitz-Gerald JM, Schroter RC*. Arterial Wall Shear and Distribution of Early Atheroma in Man. Nature 1969; 223(5211): 1159−61.
21. *Malek AM, Alper SL, Izumo S*. Hemodynamic shear stress and its role in atherosclerosis. JAMA 1999; 282(21): 2035−42.
22. *Friedman MH, Bargeron CB, Deters OJ, Hutchins GM, Mark FF*. Correlation between wall shear and intimal thickness at a coronary artery branch. Atherosclerosis 1987; 68(1−2): 27−33.
23. *Prosi M, Perktold K, Ding Z, Friedman MH*. Influence of curvature dynamics on pulsatile coronary artery flow in a realistic bifurcation model. J Biomech 2004; 37(11): 1767−75.
24. *Chatzizisis YS, Baker AB, Sukhova GK, Koskinas KC, Papafaklis MI, Beigel R*, et al. Augmented expression and activity of extracellular matrix-degrading enzymes in regions of low endothelial shear stress colocalize with coronary atheromata with thin fibrous caps in pigs. Circulation 2011; 123(6): 621−30.
25. *Koskinas KC, Sukhova GK, Baker AB, Papafaklis MI, Chatzizisis YS, Coskun AU,* et al. Thin-capped atheromata with reduced collagen content in pigs develop in coronary arterial regions exposed to persistently low endothelial shear stress. Arterioscler Thromb Vasc Biol 2013; 33(7): 1494−504.
26. *Rizik DG, Klassen KJ, Hermiller JB*. Bifurcation coronary artery disease: current techniques and future directions (part 2). J Invasive Cardiol 2008; 20(3): 135−41.
27. *Cheng C, Tempel D, van Haperen R, van der Baan A, Grosveld F, Daemen MJ*, et al. Atherosclerotic Lesion Size and Vulnerability Are Determined by Patterns of Fluid Shear Stress. Circulation 2006; 113(23): 2744−53.
28. *Schaar JA, Muller JE, Falk E, Virmani R, Fuster V, Serruys PW,* et al. Terminology for high-risk and vulnerable coronary artery plaques. Report of a meeting on the vulnerable plaque, June 17 and 18, 2003, Santorini, Greece. Eur Heart J 2004; 25(12): 1077−82.
29. *Nakazawa G, Yazdani SK, Finn AV, Vorpahl M, Kolodgie FD, Virmani R*. Pathological findings at bifurcation lesions: The impact of flow distribution on atherosclerosis and arterial healing after stent implantation. J Am Coll Cardiol 2010; 55(16): 1679−87.
30. *Zarins CK, Giddens DP, Bharadvaj BK, Sottiurai VS, Mabon RF, Glagov S*. Carotid bifurcation atherosclerosis. Quantitative correlation of plaque localization with flow velocity profiles and wall shear stress. Circ Res 1983; 53(4): 502−14.
31. *Grottum P, Svindland A, Walloe L*. Localization of atherosclerotic lesions in the bifurcation of the main left coronary artery. Atherosclerosis 1983; 47(1): 55−62.
32. *Joner M, Finn AV, Farb A, Mont EK, Kolodgie FD, Ladich E*, et al. Pathology of drug-eluting stents in humans: Delayed healing and late thrombotic risk. J Am Coll Cardiol 2006; 48(1): 193−202.
33. *Kraemer BF, Schmidt C, Urban B, Bigalke B, Schwanitz L, Koch M*, et al. High shear flow induces migration of adherent human platelets. Platelets 2011; 22(6): 415−21.
34. *Gutierrez-Chico JL, Gijsen F, Regar E, Wentzel J, de Bruyne B, Thuesen L,* et al. Differences in neointimal thickness between the adluminal and the abluminal sides of malapposed and side-branch struts in a polylactide bioresorbable scaffold: evidence

in vivo about the abluminal healing process. JACC Cardiovasc Interv 2012; 5(4): 428−35.

35. *Jimenez JM, Davies PF.* Hemodynamically driven stent strut design. Ann Biomed Eng 2009; 37(8): 1483−94.
36. *Raber L, Juni P, Loffel L, Wandel S, Cook S, Wenaweser P,* et al. Impact of stent overlap on angiographic and long-term clinical outcome in patients undergoing drug-eluting stent implantation. J Am Coll Cardiol 2010; 55(12): 1178−88.

Received on August 9, 2015.
Accepted on October 6, 2015.
Online First December, 2015.